Electronic stopping power in liquid water for protons and α particles from first principles

Kyle G. Reeves, Yi Yao, and Yosuke Kanai

Electronic Stopping Power in Liquid Water for Protons and α-particles from First Principles

Kyle G. Reeves, Yi Yao, and Yosuke Kanai

Department of Chemistry, University of North Carolina, Chapel Hill, North Carolina 27599

Atomistic calculations of the electronic stopping power in liquid water for protons and α-particles from first principles are demonstrated without relying on linear response theory. The computational approach is based on non-equilibrium simulation of the electronic response using real-time time-dependent density functional theory. By quantifying the velocity-dependence of the steady-state charge of the projectile proton and α-particle from non-equilibrium electron densities, we examine the extent to which linear response theory is applicable. We further assess the influence of the exchange-correlation approximation in real-time time-dependent density functional theory on the stopping power with range-separated and regular hybrid functionals with exact exchange.

Accurate electronic stopping power in liquid water for protons and other light ions such as α-particles is of great importance because energy dissipation from the ions is at the heart of various medical and technological applications, including proton beam cancer therapy[8]. As a highly energetic ion travels through and interacts with matter, its kinetic energy is transferred into the target material's electronic and nuclear subsystems. This energy loss of the projectile particle can arise from elastic collisions with nuclei (nuclear stopping) and inelastic scattering events (electronic stopping). When the particle's kinetic energy is sufficiently large, the majority contribution to the energy transfer is due to the electronic stopping wherein the projectile particle induces massive electronic excitations in the target material. The rate of energy transfer from the ion to electrons in the material is generally measured per unit distance travelled by the projectile particle and is referred to as electronic stopping power. This velocity-dependent quantity is of central importance to many applications. For instance, proton beam cancer therapy takes advantage of the stopping power curve, which possesses a strong peak at a specific velocity and thus can deliver a significant amount of energy to a small area of cancer cells. Being the primary component of tissue, liquid water's electronic stopping power curve is of great importance in this context. At the same time, only limited experimental measurements exist near the stopping power maximum, and various different theoretical models are currently used with empirical parameters. As discussed by Emfietzoglou and co-workers in their recent work[4], further experimental and theoretical studies in the energy range below the proton kinetic energy of 1 MeV (v= 6.27 a.u) are needed to elucidate differences among the existing analytical models based on different approximations. In this work, we present the electronic stopping power in liquid water for protons and α-particles from non-equilibrium dynamical simulations based on first-principles quantum mechanical theory.

Ever since the phenomenon of electronic stopping was conceived in the early 20th century[12-15], many have worked on calculating electronic stopping power[16-18]. Within the framework of linear response theory (consequently, the projectile ion is assumed to have a fixed charge Z), the stopping power can be expressed in a mathematically closed form as

$$S(v) = \frac{4\pi Z^2}{v^2} L(v), \tag{1}$$

where v is the projectile ion velocity, and L(v) is a velocity-dependent quantity called the stopping logarithm. Bethe derived an analytical expression for the stopping logarithm using perturbation theory in the 1930s[12], arriving at the expression

$$L(v) = N_e ln\left(\frac{2v^2}{I}\right), \tag{2}$$

where N_e is the electron number density. I is the so-called mean excitation energy of the target, and it can be calculated using electronic structure calculations or from experimental measurements of the target material's optical properties. Bethe's theory often serves as a starting point of many other models that are employed today with empirical and higher-order Z corrections. A majority of work in the community relies on this formulation with different approximations and corrections for obtaining the electronic stopping power in liquid water[21]. Lindhard alternatively expressed the stopping logarithm[22]

$$L(v) = \frac{1}{2\pi^2} \int_0^{qv} \omega \, d\omega \int_0^{\infty} \frac{dq}{q} Im\left(\frac{1}{\varepsilon(q,\omega)}\right), \tag{3}$$

where ε is the macroscopic dielectric function of frequency ω and wavelength q. This formulation is widely used with the dielectric function model by Lindhard [23] for homogeneous electron gas [24,25]. For liquid water, Emfietzoglou and co-workers have made important progress by developing accurate dielectric function models by extending the experimentally measured optical limit (i.e. q=0) to finite momentum in the last decade[4,26].

Real-time time-dependent density functional theory (RT-TDDFT)[27] has advanced rapidly for studying the non-equilibrium response of quantum systems in the last several years, and a few groups have started to explore the use of RT-TDDFT for obtaining electronic stopping power by directly simulating the electronic response to the projectile ion. Artacho and co-workers successfully demonstrated this approach initially for obtaining the electronic stopping power in low velocity regime (below the maximum) [28,29], and it also appeared promising for obtaining stopping power curves even for higher ion velocities[30]. By developing a highly-scalable implementation of the RT-TDDFT method using a plane-wave basis[31,32], we demonstrated that electronic stopping can be accurately modeled over a wide range of velocities including the stopping power maximum for a representative metallic system of aluminum[33] for which many experimental measurements exist. For liquid water, however, a
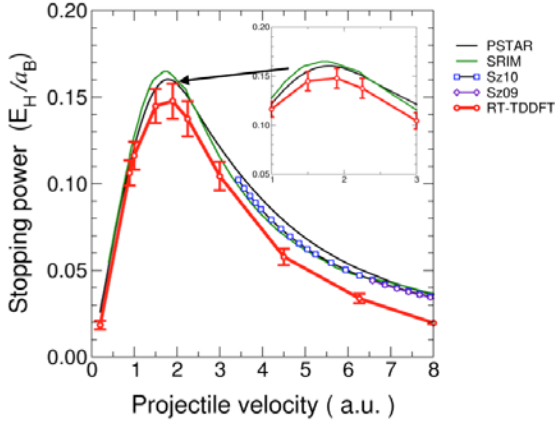
FIG. 1. Electronic stopping power curves for a proton in liquid water. Two widely-used empirical models, PSTAR[1] (black) and SRIM[2] (green), are shown for comparison. Experimental data based on work by Sz09[6] and Sz10[11] are shown as blue squares and purple diamonds, respectively. Our real-time TDDFT results are shown as the red line, and the error bars represent standard deviations for the path distribution.
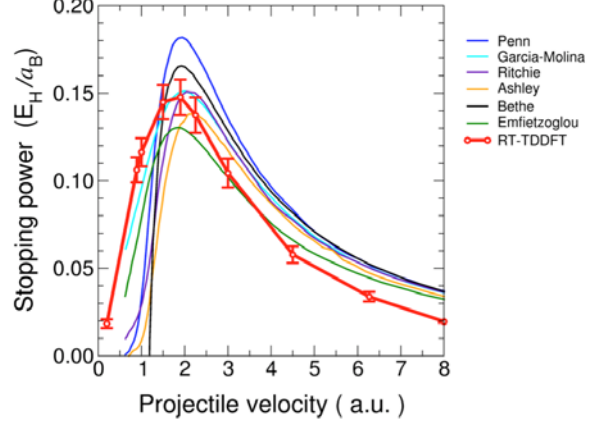

FIG. 2. Analytical models of electronic stopping power and our real-time TDDFT results for a proton in liquid water. Analytical model using various model dielectric functions by Garcia-Molina[3] (cyan), Penn (blue), Ritchie (purple), Ashley (orange), and Emfietzoglou (green) are shown for comparison [4]. Bethe theory (black) is also shown with the mean excitation energy of I=75 eV as recommended by the International Commission on Radiation Units and Measurement[7]. Our real-time TDDFT results are shown as the red line, and the error bars represent standard deviations for the path distribution.

limited number of experimental measurements are available for protons despite its medical and technological importance, and those data exist only for very high velocities away from the stopping power maximum. Thus, the analytical models remain unconfirmed in the velocity range around the anticipated stopping power peak. In the case of α-particles, two existing experiments show distinctly different behavior near the stopping power maximum. While the two widely used empirical SRIM[2] and PSTAR[1] models agree quite closely, analytical models based on model dielectric functions vary substantially among themselves [4].

Using our recently developed, highly-scalable RT-TDDFT method in QB@LL code[34], non-equilibrium simulations are performed to obtain the dynamical electronic response of liquid water to an energetic ion (proton and α-particle). The details of the RT-TDDFT implementation are discussed in Ref. [31] and Ref. [32], and the non-equilibrium simulation approach for calculating the electronic stopping power is presented in Ref. [33]. We calculate the electronic stopping power (energy transfer rate) via

$$S(v) = \langle \frac{dE[\rho(r;t)]}{dx} \rangle_v, \qquad (4)$$

where E is time-dependent electronic energy[33] and x is the projectile ion position. The energy derivative is obtained for individual paths using a baseline fitting approach[35], and the classical ensemble average is taken over projectile paths with a constant projectile ion velocity. In the present case of liquid water, at least 10 projectile paths were used for each projectile ion velocity. A first-principles molecular dynamics (FPMD) simulation was performed first to obtain a representative structure of liquid water at room temperature, using 162 water molecules (1,296 electrons) in a cubic simulation cell (16.229 Å) with periodic boundary conditions, following Ref. [36]. The positions of water molecules were taken from a snapshot of an equilibrated trajectory of a 20-picoseconds FPMD simulation. For the RT-

TDDFT simulations, a small time step of 0.2 attoseconds was used to ensure strict convergence. The PBE XC functional was used within adiabatic approximation[37,38]. A plane-wave cuttoff of 50 Ryd at gamma point only in Brillouin zone integration was sufficient due to the large simulation cell with 162 water molecules. Hamann-Schluter-Chiang-Vanderbilt norm-conserving pseudo-potentials were used[39], and 1s electrons of oxygen atoms are treated as core electrons within the pseudopotential. Previous work has shown that core electrons contributes < 5% to the stopping power below v=6.27 a.u and essentially none near the stopping power maximum at v=1.98 a.u.[40].

Fig. 1 shows the electronic stopping power from our RT-TDDFT simulation, in comparison to the two widely used empirical SRIM and PSTAR models, in addition to available experimental measurements for high proton velocities. The error bars for our RT-TDDFT result represent standard deviations based on the distribution of projectile ion paths, and the dependence of the stopping power on the proton path was found to be more significant near the stopping power maximum. SRIM and PSTAR agree quite well near the stopping power maximum with $v_{proton} = 1.7$ a.u. and 1.8 a.u. respectively, and our first-principles simulation predicts the location of the maximum at 1.9 a.u. At the same time, our simulations yield a lower stopping power value with respect to these models, and our results underestimate the experimental values at higher velocities. We also compared our first-principles result to theoretical models that are based on Bethe theory (Eq. (2)) and the dielectric function formalism (Eq. (3)) in Fig. 2. These analytical models generally show a much steeper curve at lower velocities than the empirical SRIM and PSTAR models. Bethe theory shows a qualitatively incorrect behavior below the stopping power maximum due to the logarithmic term (See Eq. (2)). The dielectric function formulation generally contains the energy loss function $Im(-\varepsilon^{-1}(q, \omega))$, and the experimental measurement of the optical limit (q=0) can be extended into a finite momentum q≠0. Recent work by Emfietzoglou and co-workers has investigated the dependence on
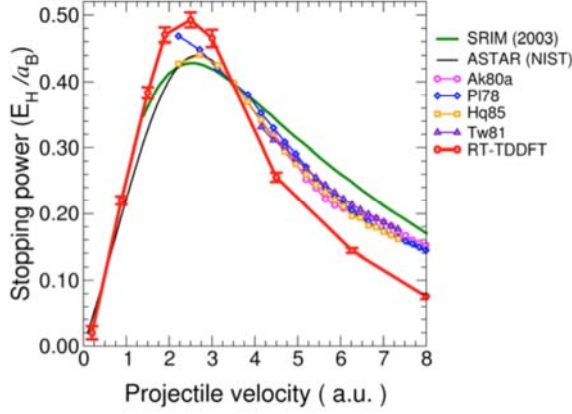
FIG. 3. Stopping power curves for a α-particle in liquid water. Two widely-used empirical models, SRIM[2] (green line) and ASTAR[1] (black line) are shown for comparison to our real-time TDDFT results (red line). Experimental data for stopping power curves Ak80a (magenta circles, Ref. [9]), Pl78 (blue diamond, Ref. [6,10,11]), Hq85 (yellow squares, Ref. [19]), and Tw81 (purple triangles, Ref. [20]) are shown.

FIG. 4. Mean steady-state charge ($\bar{q}$) for a proton (left) and an α-particle (right) in liquid water as a function of the projectile ion velocity. Error bars represent the standard deviations of the distribution of the instantaneous charge state, which is calculated using the Voronoi partitioning in the simulation (see text). The empirical model for projectile charge-state by Schiwietz and Grande is shown in the dashed line[5].

different model dielectric functions[4]. Notably, Ritchie *et al.* proposed a model based on the random phase approximation, exhibiting a quadratic dependence on q[41]. Ashley and Penn utilized a plasmon-pole approximation for their momentum dispersion schemes to extend the optical limit[42,43]. Alternatively, Emfietzoglou proposed an extended Drude-type model by introducing an empirical correction function for the q dependence[26]. The model by Garcia-Molina, et al. relies on the dielectric function due to Mermin, for the momentum dependence[3]. In addition to specifying the dielectric function, these analytical models are augmented by higher order corrections in Z and/or by employing an effective charge state model for the proton charge such as that of Brandt and Kitagawa[44,45] and of Schiwietz and Grande[5], which is more widely used for liquid water[3]. As can be seen in Fig. 2, the stopping power maximum varies significantly among these different analytical models while the locations of the maximum all fall in 1.7 ~ 2.1 a.u. Our first-principles simulation result predicts a more gradual decay of the stopping power from the maximum to lower velocities than these models as in SRIM and PSTAR empirical models.

Linear response theory predicts the quadratic dependence of the electronic stopping power (i.e. energy transfer rate) on the projectile ion charge as discussed in the introduction, and thus the use of α-particles instead of protons is also of great interest for various medical/technological applications such as for cancer therapies[8]. The electronic stopping power for α-particles is shown in Figure 3, and SRIM and ASTAR[1] empirical models agree rather closely near the maximum, and our first-principles RT-TDDFT result predicts the location of the expected maximum in good agreement. However, the stopping power value itself is much higher than these empirical models. For α-particles, there exist two different sets of experimental measurements near the maximum, and their behaviors differ quite significantly. The velocity-dependent trend of our first-principles results follows more closely of experimental measurement by Haque *et al.* (Hq85, Ref. [19]) rather than the one measured by Palmer *et al.* (Pl75, Ref. [10]) although there remains much room for improvement in
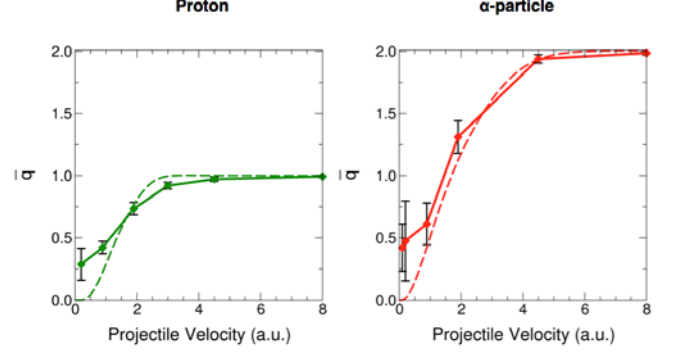
obtaining better accuracy from first-principles theory as discussed later.

Most widely-used analytical models involve augmenting a linear response theory description with empirical higher order corrections and/or by employing an effective charge model for the projectile ion charge, making the approach more empirical and susceptible to the problem of adjusting many interdependent parameters [46,47]. Within linear response theory, one starts by considering a particle with a fixed charge interacting with a matter. A result of this theoretical treatment is the quadratic dependence of the stopping power on the projectile ion charge as seen in both Bethe theory and Lindhard formula. We now ask to what extent linear response theory can describe the electronic stopping power without higher order corrections. Specifically, we explore if its description can be improved if the velocity-dependent charge state of the projectile ion from our non-equilibrium simulations is used instead of assuming a fully-ionized projectile ion. To answer this question, we calculate the mean steady-state charge of the projectile ion in liquid water by employing a Voronoi partitioning scheme[48] in which the cell of a given atom is defined as the region of space closer to the given atom than to any other atoms. In crystalline materials, the Voronoi cell is equivalent to the Wigner-Seitz cell. This approach provides an ideal partitioning scheme for the projectile ion in this context because this geometric criterion does not depend on the non-equilibrium density and the definition of each cell is therefore independent of the projectile ion velocity. To calculate the charge of the projectile ion from its Voronoi cell, the equilibrium electron density is first subtracted from the velocity-dependent, non-equilibrium electron density so that the electron density of liquid water does not contribute to the projectile ion charge. Fig. 4 shows the calculated mean-steady state charge of the projectile ion as a function of the velocity from our non-equilibrium RT-TDDFT simulations. The charge on the projectile ion increases as the ion velocity increases as expected, and both protons and α-particles can be considered as bare ions by v=~8 a.u.. At very low velocities, neither protons nor α-particles are a completely neutral species as described in typical effective charge
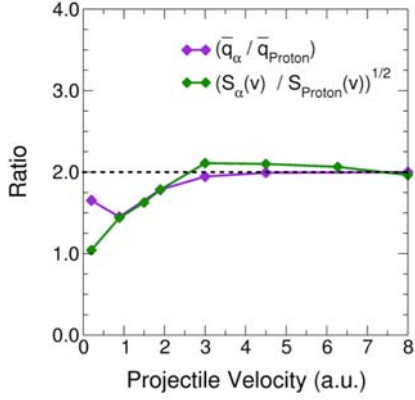
FIG. 5. Velocity-dependent ratios between protons and α-particles for calculated stopping power and projectile ion charge state in liquid water. The ratio of the calculated electronic stopping power curves is shown as green diamonds. The ratio of the effective charge on each projectile is plotted as purple diamonds. The dashed line represents the stopping power ratio of 2, which is expected from linear response theory when assuming fully ionized charges.

models[44,45]. Fig. 5 shows the comparison of the stopping power ratio, $(S_\alpha/S_{proton})^{1/2}$, to the mean steady-state ion charge ratio, q_α/q_{proton}, as a function of the velocity. At the velocity of ~8 a.u., the stopping power ratio reaches the value of 2 for α-particle/proton as one would expect from assuming fully-ionized charges in linear response theory (i.e. $(S_\alpha/S_{proton})^{1/2}=Z_\alpha/Z_{proton}$). By simulating the non-equilibrium electronic dynamics explicitly, the RT-TDDFT approach captures the non-linearity in the response as, at lower projectile velocities, first-order perturbation theory begins to fail. Interestingly, $(S_\alpha/S_{proton})^{1/2}$ follows rather closely to the ratio q_α/q_{proton} even for low ion velocities below the stopping power maximum down to ~1 a.u.. Thus, linear response behavior is found to be followed rather closely for the present case of liquid water when the mean steady-state charge state is used instead of assuming fully-ionized charges over a rather wide range of velocities or in other words contributions from higher-order Z-terms are dominated by changes to the mean steady-state charge of the projectiles.

Finally, we remark on the approximated exchange-correlation (XC) potential used in the RT-TDDFT simulations[49].
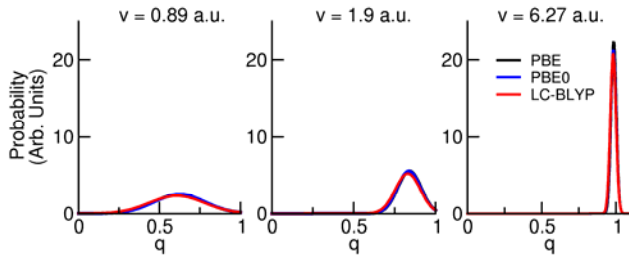

FIG. 6. Normalized Gaussian distributions for the probability of observing a projectile proton with an instantaneous charge state, q, in liquid water. Proton velocities of v = 0.89 a.u. (left), v = 1.9 a.u. (center), and v = 6.27 a.u. (right) were simulated using three different exchange-correlation functionals: PBE (black), PBE0 (blue) and LC-BLYP (red).

TABLE I. Percentage difference in the calculated electronic stopping power in liquid water for proton using two hybrid exchange-correlation approximations (PBE0 and LC-BLYP) with respect to GGA approximation (PBE).

	PBE0	LC-BLYP
v = 0.89 a.u.	-5.7%	-2.4%
v = 1.9 a.u.	-1.0%	8.4%
v = 6.27 a.u.	1.9%	3.1%

First, we adapted the adiabatic approximation such that XC potential depends on the instantaneous electron density, neglecting any potential memory effects[38]. By calculating the linear part of the stopping power in the low ion velocity limit for a homogeneous electron gas (i.e. friction coefficient) using time-dependent current DFT formulation, Nazarov and co-workers have shown that the adiabatic approximation results in a negligibly small error when the projectile ions are of low-Z elements like protons and α-particles [50]. Second, the semi-local approximation like GGA-PBE[37] used here for the XC potential might introduce errors, especially since dynamical charge transfer between the ion and target could be important for some projectile ion velocities. Employing the hybrid functional PBE0[51] and range-corrected hybrid XC functional LC-BLYP[52], we examined differences with the PBE result at v_{proton}= 0.89, 1.90, and 6.27 a.u.. In our recent work, LC-BLYP functional was found to perform quite satisfactorily in describing a long-range charge transfer in comparison to reptation quantum Monte Carlo and coupled cluster calculations[53]. For examining the XC dependence of the electronic stopping power, we used a Gaussian basis set instead of a plane-wave basis due to the prohibitively large computational cost of using plane-wave basis for these hybrid functionals in the present context. The range-corrected hybrid GGA (LC-BLYP) was implemented in CP2K code[54] using libxc library[55] for our RT-TDDFT calculation. TZV2P Gaussian basis set was used with Goedecker-Teter-Hutter pseudopotentials for core electrons[56]. The exact exchange in PBE0 and LC-BLYP functionals was computed using the auxiliary density matrix method with cFIT3 auxiliary basis set[57]. Crank-Nicholson method was used to propagate the Kohn-Sham wavefunctions with a timestep of 0.24 attoseconds. In some parts of the simulations, the time step had to be reduced to 0.06 attoseconds to perform a stable numerical integration. For velocities that are less than, equal to, and greater than the peak velocity, the choice of XC functional makes very little difference in the calculated instantaneous charge state of the projectile proton in liquid water as seen in Figure 6. Table 1 shows percentage deviation in calculated stopping power with respect to the PBE result for a single representative proton trajectory. All deviations are within 10%, and the LC-BLYP approximation showed the largest change of +8.4% at v_{proton}= 1.90 a.u., the stopping power maximum. These appreciable variations indicate that XC approximation needs to be improved in our RT-TDDFT simulations for obtaining quantitatively accurate determination of electronic stopping power from first-principles theory.

In conclusion, we determined electronic stopping power in liquid water for protons and α-particles from first-principles theory using RT-TDDFT simulations, without empirical parameters or relying on linear response theory. The calculated stopping power curves were compared to both SRIM and P(A)STAR empirical models as well as to analytical theories based on model dielectric functions. Our parameter-free calculation of the stopping power curve supports a good level of reliability of the empirical models for liquid water, and it also shows that the analytical models predict a stopping power curve that decreases too rapidly from its maximum in the low ion velocity regime. At the same time, our first-principles RT-TDDFT results appear to somewhat underestimate the experimental measurements for large velocities, and further studies are needed on the role of the exchange-correlation approximation. Lastly, we found that the stopping power ratio, $(S_\alpha/S_{proton})^{1/2}$, deviates significantly from the expected value of 2 from linear response theory in the ion velocity regime below ~3 a.u.. However, down to the velocity of ~1 a.u., this can be largely rectified for the present case of liquid water if the mean steady-state charge from our RT-TDDFT non-equilibrium simulations is used instead of assuming fully-ionized charges for the projectile ions. Given significant uncertainty in fitting analytical models with higher-order corrections [46,47], this result provides a rigorous physical bound that should be employed in developing empirical models for the effective charge state.

References

[1] M. J. Berger, J. S. Coursey, M. A. Zucker, and J. Chang, National Institute of Standards and Technology, Gaithersburg, MD (2005).

[2] J. F. Ziegler, M. D. Ziegler, and J. P. Biersack, Nucl Instrum Meth B **268**, 1818 (2010).

[3] R. Garcia-Molina, I. Abril, P. de Vera, I. Kyriakou, and D. Emfietzoglou, Appl Radiat Isotopes **83**, 109 (2014).

[4] D. Emfietzoglou, R. Garcia-Molina, I. Kyriakou, I. Abril, and H. Nikjoo, Phys Med Biol **54**, 3451 (2009).

[5] G. Schiwietz and P. L. Grande, Nucl Instrum Meth B **175**, 125 (2001).

[6] M. Shimizu, M. Kaneda, T. Hayakawa, H. Tsuchida, and A. Itoh, Nucl Instrum Meth B **267**, 2667 (2009).

[7] I. C. o. R. U. a. Measurements, International Commission on Radiation Units and Measurements, Stopping powers and ranges for electrons and positrons, Report No. 37, (1984).

[8] W. D. Newhauser and R. Zhang, Phys Med Biol **60**, R155 (2015).

[9] A. Akhavan-Rezayat and R. B. J. Palmer, Journal of Physics E: Scientific Instruments **13**, 877 (1980).

[10] R. B. J. Palmer and A. Akhavan-Rezayat, J. Phys. D: Appl. Phys. **11**, 605 (1978).

[11] M. Shimizu, T. Hayakawa, M. Kaneda, H. Tsuchida, and A. Itoh, Vacuum **84**, 1002 (2010).

[12] H. Bethe, Annalen der Physik **397**, 325 (1930).

[13] M. Born and R. Oppenheimer, Annalen der Physik **389**, 457 (1927).

[14] J. J. Thomson, Philosophical Magazine Series 6 **23**, 449 (1912).

[15] C. G. Darwin, Philosophical Magazine Series 6 **23**, 901 (1912).

[16] M. Inokuti, Reviews of Modern Physics **43**, 297 (1971).

[17] E. Fermi and E. Teller, Physical Review **72**, 399 (1947).

[18] C. P. Race, D. R. Mason, M. W. Finnis, W. M. C. Foulkes, A. P. Horsfield, and A. P. Sutton, Reports on Progress in Physics **73**, 116501 (2010).

[19] A. K. M. M. Haque, A. Mohammadi, and H. Nikjoo, Radiation Protection Dosimetry **13**, 71 (1985).

[20] D. I. Thwaites, Phys Med Biol **26**, 71 (1981).

[21] Adv Quantum Chem **65**, 1 (2013).

[22] J. Lindhard, Mat Fys Medd Dan Vid **28**, 1 (1954).

[23] G. F. V. G. Giuliani, *Quantum Theory of the Electron Liquid* (Cambridge, 2005).

[24] J. Lindhard and M. Scharff, Physical Review **124**, 128 (1961).

[25] P. M. Echenique, R. M. Nieminen, J. C. Ashley, and R. H. Ritchie, Physical Review A **33**, 897 (1986).

[26] D. Emfietzoglou, F. A. Cucinotta, and H. Nikjoo, Radiat Res **164**, 202 (2005).

[27] E. Runge and E. K. U. Gross, Phys Rev Lett **52**, 997 (1984).

[28] J. M. Pruneda, D. Sánchez-Portal, A. Arnau, J. I. Juaristi, and E. Artacho, Physical Review Letters **99**, 235501 (2007).

[29] M. A. Zeb, J. Kohanoff, D. Sánchez-Portal, A. Arnau, J. I. Juaristi, and E. Artacho, Physical Review Letters **108**, 225504 (2012).

[30] A. A. Correa, J. Kohanoff, E. Artacho, D. Sánchez-Portal, and A. Caro, Physical Review Letters **108**, 213201 (2012).

[31] A. Schleife, E. W. Draeger, V. M. Anisimov, A. A. Correa, and Y. Kanai, Comput Sci Eng **16**, 54 (2014).

[32] A. Schleife, E. W. Draeger, Y. Kanai, and A. A. Correa, J Chem Phys **137** (2012).

[33] A. Schleife, Y. Kanai, and A. A. Correa, Physical Review B **91**, 014306 (2015).

[34] E. W. Draeger and F. Gygi, Lawrence Livermore National Lab, Qbox (Qb@ll Branch), tech. report, (2014).

[35] H. F. M. Boelens, R. J. Dijkstra, P. H. C. Eilers, F. Fitzpatrick, and J. A. Westerhuis, J Chromatogr A **1057**, 21 (2004).

[36] J. C. Grossman, E. Schwegler, E. W. Draeger, F. Gygi, and G. Galli, J Chem Phys **120**, 300 (2004).

[37] J. P. Perdew, K. Burke, and M. Ernzerhof, Phys Rev Lett **77**, 3865 (1996).

[38] N. T. Maitra, K. Burke, and C. Woodward, Phys Rev Lett **89** (2002).

[39] D. Vanderbilt, Phys Rev B **32**, 8412 (1985).

[40] D. Emfietzoglou, H. Nikjoo, and A. Pathak, Nucl Instrum Meth B **249**, 26 (2006).

[41] R. H. Ritchie, Nucl Instrum Methods **198**, 81 (1982).

[42] J. C. Ashley, J Phys-Condens Mat **3**, 2741 (1991).

[43] D. R. Penn, Phys Rev B **35**, 482 (1987).

[44] W. Brandt, Nucl Instrum Methods **194**, 13 (1982).

[45] W. Brandt and M. Kitagawa, Phys Rev B **25**, 5631 (1982).

[46] L. E. Porter, Int J Quantum Chem **95**, 504 (2003).

[47] R. Cabrera-Trujillo, J. R. Sabin, and J. Oddershede, Phys Rev A **68** (2003).

[48] C. F. Guerra, J. W. Handgraaf, E. J. Baerends, and F. M. Bickelhaupt, J Comput Chem **25**, 189 (2004).

[49] C. A. Ullrich, *Time-Dependent Density-Functional Theory, Concepts and Applications* (Oxford Graduate Texts, 2011).

[50] V. U. Nazarov, J. M. Pitarke, Y. Takada, G. Vignale, and Y. C. Chang, Physical Review B **76**, 205103 (2007).

[51] J. P. Perdew, M. Emzerhof, and K. Burke, J Chem Phys **105**, 9982 (1996).

[52] H. Iikura, T. Tsuneda, T. Yanai, and K. Hirao, J Chem Phys **115**, 3540 (2001).

[53] Y. Yao and Y. Kanai, Chem Phys Lett **618**, 236 (2015).

[54] J. Hutter, M. Iannuzzi, F. Schiffmann, and J. VandeVondele, Wires Comput Mol Sci **4**, 15 (2014).

[55] M. A. L. Marques, M. J. T. Oliveira, and T. Burnus, Comput Phys Commun **183**, 2272 (2012).

[56] S. Goedecker, M. Teter, and J. Hutter, Phys Rev B **54**, 1703 (1996).

[57] M. Guidon, J. Hutter, and J. VandeVondele, J Chem Theory Comput **6**, 2348 (2010).